Modeling thermal contact resistance at the finger-object interface

Konrad Rykaczewski[*]

School for Engineering of Matter, Transport and Energy, Arizona State University, Tempe, AZ, 85287, US

Keywords: contact resistance, modeling, skin, soft materials

*Corresponding author email: konradr@asu.edu

Thermal contact resistance at the finger-object interface plays a significant role in our thermal perception and is an important parameter for the design of a myriad of electronics and thermal devices. Currently, its value is measured experimentally or, more commonly, is estimated using a semi-empirical model. This model was developed by Cooper, Mikic, and Yovanovich (CMY) in the 1960s for predicting contact resistance of metal-metal interfaces in a vacuum. In this work, it is shown that measured value of finger-object contact resistance is better predicted by a more recent correlation by Prasher and Matayabas (PM) that was developed by fitting contact resistance data for silicone gel-metal surface interfaces in microelectronic applications. Furthermore, it is show that the functional form of the empirical PM correlation can be derived using scale analysis of the finger-solid contact scenario, consequently can be considered a physics-based model. Comparing the two models against two previously published experimental data sets demonstrates that the PM model predicts well the thermal resistance between finger and variety of materials over a wide range of contact pressures. Specifically, for finger contact with significantly more conductive materials (thermal conductivity above 1 $Wm^{-1}K^{-1}$) including aluminum, BaF_2 crystal, and marble a good prediction of contact resistance can be attained. For skin contact with less conductive materials, such as wood, both models become highly sensitive to the substrate's thermal conductivity value and provide only an order of magnitude estimate. The main implications of these results and relevant outstanding questions are also briefly discussed.

"Don't touch that, it's hot!" is a phrase everyone has exclaimed at some point, often to a child who neglects these wise words and proceeds to test the said statement to a painful conclusion. Interestingly, how "hot" or "cold" an object feels not only depends on its temperature in respect to that of the skin, but as recently reviewed by Hsin-Ni Ho [1] in this journal, also on a surprising number of parameters involved in physical, perceptual, and cognitive responses. One common observation that highlights the role of thermophysical properties is that metal objects feel colder than glass or plastics at the same temperature [1,2]. Additionally, we know that, to a certain degree, an object will feel hotter or colder when we press on it harder, which highlights the dependence of skin temperature on imposed contact force, F. From these observations we can infer that despite the skin and the object being in physical contact, their respective surface temperatures are not equal. The schematic in Figure 1a illustrates that this temperature jump, ΔT_c, is a result of microscopic surface roughness that reduces the contact area for heat transfer at the skin-object interface. Since the magnitude of ΔT_c depends on the heat flux between the two objects, $q"$, interfaces are typically characterized in terms of their thermal contact resistance, R_c. Based on our everyday tactile observations described above, we can expect that R_c depends on surface roughness, applied force, as well as mechanical and thermal properties of the skin and the contacting material. Since quantifying the contact resistance is important for design of electronics [2–6], thermal displays [7], artificial hands [8], haptic devices [9], and wearable thermoelectric devices [10,11], it is important to know how to combine these physical parameters to model the value of R_c.

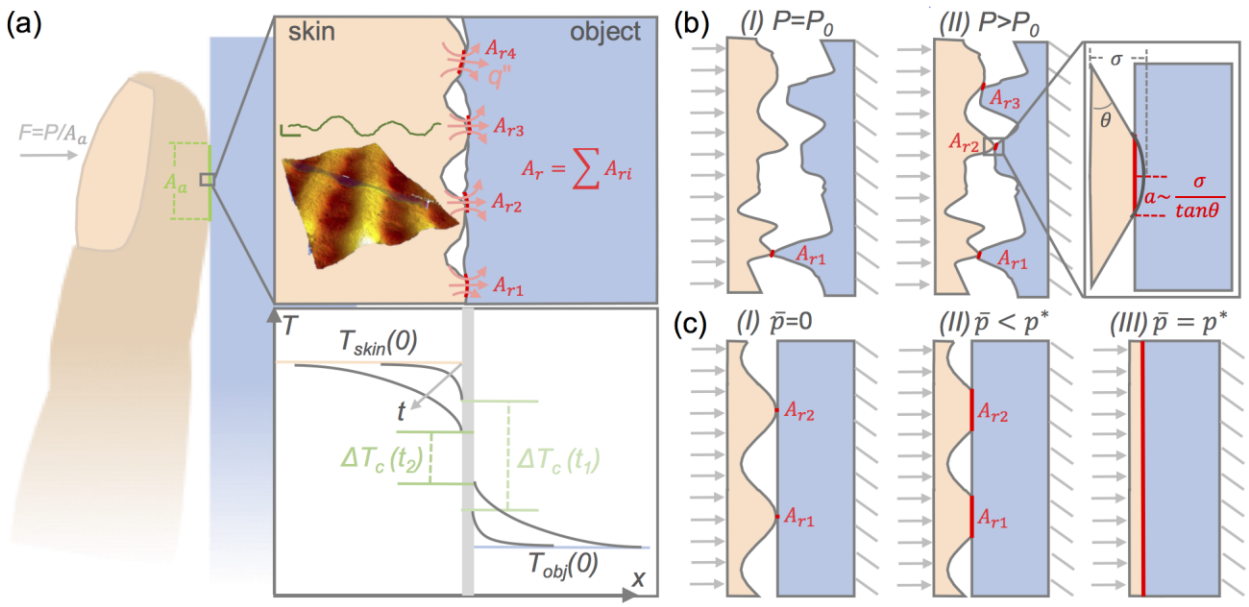

Figure 1. (a) Schematic of heat transfer at finger-object interface (inspired by work of Ho [1]). The close-up schematic and corresponding plot show that surface roughness leads to reduced heat transfer area, thus reduced heat flux q", and a temperature jump at the interface ΔT_c that reduces with time, t (F indicates the applied force, A_a indicates the apparent area, and A_r indicates the real contact area, which is a sum of the areas of the microscopic contacts, A_{ri}); a three dimensional optical scan of a replica of a male finger surface and corresponding line trace are also included (vertical and horizontal scale bars on the line trace correspond to 20 and 200 μm, respectively); (b) and (c) schematic of microscale contact geometry during (b) plastic deformation of contacting surfaces with random surface rough assumed in CMY model (a indicates circular contact radius, σ mean surface height, $tan\theta$ mean surface asperity slope) and (c) elastic deformation of one-dimensional wavy surface in contact with a stiff and flat substrate assumed to derive the functional form of PM model ($\bar{p}$ indicates mean pressure and p^* pressure at which gaps fully collapse on such surface).

The most commonly utilized model for predicting R_c at finger-object interfaces [7,9,20,12–19] was developed in the 1960s by Cooper, Mikic and Yovanovich (CMY) to predict thermal contact resistance between two contacting materials (subscript 1 and 2) with random surface roughness that are much harder than skin (e.g. metals and ceramics) in a vacuum environment [21–23]. More recently, Bahrami working with Yovanovich [24] derived the functional form of the CMY model based on scale analysis, which will be briefly reiterated here. The principle assumption of the CMY model is that deformation of most contact areas between metallic surfaces is predominantly plastic, even at moderate contact pressures. To model how this plastic deformation translates into increased interfacial contact area, the authors assumed that pressure at each contact is equal to the maximum pressure which can be sustained by the softer of the materials during plastic deformation. To quantify this value, they adopted simple assumption introduced by Holm [25]: the pressure under contact is equal to the microhardeness of the softer material, H, that is obtained from indentation tests using an indenter comparable in size to that of the microscopic contacts areas. From this assumption one can deduce the simple force balance $F = PA_a = HA_r$, from which a relation between the apparent, A_a, and the real, A_r, contact areas can be obtained as a function of the apparent contact pressure and microhardness [26]:

$$\frac{A_a}{A_r} = \frac{H}{P} \tag{1}$$

In turn, the schematics in Figure 1a and 1b show that the real contact area is a sum of n_p individual contact points, that can be idealized as circular areas with mean radius a (i.e. $A_r \approx n_p \pi a^2$). Combining of these two expressions yields a formula for the number of contact points:

$$n_p \approx \frac{A_a P}{\pi a^2 H} \tag{2}$$

The key implication of Equation 2 is that for contact of two metal surfaces with random surface roughness the number of contact points increases linearly with pressure, while their mean size

remains roughly unchanged (i.e. πa^2). The schematic on right hand side of Figure 1b shows that simple geometry can be used to show that $a \sim \sigma/m$, where $\sigma = \sqrt{\sigma_1^2 + \sigma_2^2}$ is the equivalent root-mean square roughness (used as a measure of mean surface asperity height) and $m = \sqrt{m_1^2 + m_2^2}$ is the equivalent asperity slope that is equal to tangent of the mean asperity angle θ ($m = tan\theta$). Bahrami *et al*. [24] showed that on typical surfaces the contact points are separated sufficiently far enough that the spreading thermal resistance from material 1 to material 2 can be approximated as a small heat source on an semi-infinite medium, for which spreading resistance is equal to:

$$R_{c-p} = \frac{1}{2ak_s} = \frac{1}{4a\frac{k_1 k_2}{k_1+k_2}} \tag{3}$$

Where inclusion of the harmonic mean thermal conductivity ($k_s = 2k_1k_2/(k_1+k_2)$) stems from summation of the two spreading resistances in series. Since the total contact resistance consists of n_p such sources that conduct heat in parallel, the total contact resistance scales with R_{c-p}/n_p. Substituting the previously discussed geometrical relation for a and Equation 2 as well as multiplying by the apparent area yields final expected functional form of the total contact resistance of two rough metal surfaces for a unit area of the interface (R''_{c-CMY} in units of m^2KW^{-1}) [24]:

$$R''_{c-CMY} \sim \frac{A_a}{2ak_s n_p} \sim \frac{A_a}{2ak_s\frac{A_a P}{\pi a^2 H}} \sim \frac{\pi}{2k_s}\frac{\sigma}{m}\frac{H}{P} \tag{4}$$

Substituting the scaling factors into Equation 4 obtained from fitting of experiments yields the most commonly used form of the CMY model [24]:

$$R''_{c-CMY} = \frac{4}{5k_s}\frac{\sigma}{m}\left(\frac{H}{P}\right)^{0.95} \tag{5}$$

Even in the original paper, CMY [21] acknowledged that Equation 5 was a big simplification and that, from a mechanical point of view, ignores possible effects of previous contacts, creep,

thermal induced deformations, etc. Despite these simplifications, the CMY model agrees well with measured values of thermal contact resistance for many contacting hard surfaces [24,26].

In adopting Equation 5 for contact resistance calculations between a human finger and a barium fluoride (BaF_2) crystal, Ho and Jones [27] acknowledged that this model has a rather limited ability to predict this value for a soft-hard material interface under the application of light pressure in the range of 1 to 10 kPa (Equation 5 is valid for P of 35 to 350 kPa). In 1997, Parihar and Wright [28] brought up similar concerns about the adequacy of Equation 5 for predicting contact resistance of an elastomer-metal interface. A few years later, Prasher and Matayabas (PM), who were working on the development of soft thermal interface materials for integrated circuit packaging, addressed this issue directly [29]. Specifically, the authors developed an empirical correlation for predicting thermal contact resistance between polished metal surfaces and soft silicone gels with shear moduli in the range of 1 to 460 kPa. As these silicones were gels the authors found it impossible to measure their microhardness and instead utilized their storage (G') and loss (G'') shear moduli, which were measured at low frequency and strain rate (plate rotational rate of 1 rad/s at constant strain of 10%), as the characteristic mechanical properties. PM adopted the functional form of CMY model (Equation 4) but replaced the original empirical coefficients with ones that they obtained from fitting the experimental data for silicone gels. Since in microelectronic packages thermal interface materials are in contact with much more thermally conductive materials, such as a silicon wafer and a metal heat spreader or a heat sink, PM assumed that $k_2 \gg k_1$ and simplified the value of k_s to $2k_1$ ($k_s = 2k_1k_2/(k_1+k_2) \approx 2k_1$). The authors also implicitly assumed that the silicone gel is smooth as compared to the metal surface, consequently $\sigma = (\sigma_2^2)^{0.5} \approx \sigma_2 \approx 1$ μm. With these simplification, they proposed the following expression, referred to as the PM correlation from now

on, for predicting contact resistance between soft silicones (material 1) and hard, thermally conductive materials (material 2) [29,30]:

$$R''_{c-PM} = 83.8\frac{\sigma}{k_1}\left(\frac{G_1}{P}\right)^{\frac{1}{4}} \quad (6)$$

Where $G = (G'^2 + G''^2)^{0.5}$ is the equivalent shear modulus, while k_1 is the thermal conductivity of the silicone gel. Note that the prefactor of two stemming from the mean harmonic thermal conductivity simplification (i.e. $k_s \approx 2k_1$) is incorporated into the PM correlation prefactor. At low frequency human skin has $G'_{skin} \approx 0.4 \pm 0.1$ kPa and $G''_{skin} \approx 0.1 \pm 0.02$ kPa (68% confidence interval) [31], which makes $G_{skin} \approx 0.41 \pm 0.1$ kPa just slightly below the lower bound of the range measured by PM (1 kPa) [29]. Thus, it is plausible that PM correlation could provide a better prediction of the contact resistance of a finger-metal interface than the classical CMY model. Moreover, we show next that the functional form of PM correlation can be derived from scale analysis of a physical scenario approximating finger contact with a harder and smoother material.

The primary feature a finger surface is that it consists of periodic shallow ridges that, on micro-to-millimeter level, could be idealized as a soft elastic solid with a wavy, periodic one-dimensional sinusoidal surface (see example topographical image and line trace of replica of an adult male finger obtained using optical profilometry in Figure 1a, associated experimental details in Supplemental Material, and the schematics in Figure 1c). The one-dimensional assumption is valid because the wavelength, $\lambda \approx 0.5$ mm, of the ridges is much shorter than their typical length, $L \gg 1$ mm. Consequently, pushing a flatter and stiffer solid against this idealized surface results in formation of parallel contact strips, through which heat is conducted. Johnson showed that contact between such one-dimensional sinusoidal surface with wavelength λ and amplitude 2Δ (i.e. height distribution $\Delta\,(1 - cos2\pi x/\lambda)$ and, upon contact, pressure distribution $\bar{p} + p^* cos2\pi x/\lambda$) and

harder, and much flatter, surface results in ratio of real (strips with width of $2a$ and length L) and apparent contact areas of [32]:

$$\frac{A_r}{A_a} = \frac{2aL}{\lambda L} = \frac{2a}{\lambda} = \frac{2}{\pi} sin^{-1}\sqrt{\frac{\bar{p}}{p^*}} \approx \frac{2}{\pi}\sqrt{\frac{\bar{p}}{p^*}} \quad (7)$$

Where the simplification on the right-hand side of Equation 7 is valid for small deformations that occur for $\bar{p}/p^* \leq 0.25$. The schematic in Figure 1c shows that $\bar{p}$ is the mean pressure (per A_a) and p^* is pressure at which the interfacial gaps fully collapse. The latter parameter is equal to:

$$p^* = \frac{\pi E^* \Delta}{\lambda} = \frac{\pi \Delta}{\lambda}\left(\frac{1-\nu_1^2}{E_1} + \frac{1-\nu_2^2}{E_2}\right)^{-1} \quad (8)$$

Where E and υ correspond to the Young's modulus and the Poisson's ratio of the contacting materials 1 and 2. The key implication of Equations 7 and 8 is that the number of contact strips within an area, $n_s = A_a/\lambda L$, remains constant but each strip's area increases as the contact pressure is increased. This is the principal distinguishing feature from the CMY model, in which plastic deformation assumption translates into a constant mean contact point area, but increasing number of contacts with increasing contact pressure (see Equation 2 and Figure 1b).

From heat transfer perspective, Yovanovich and Marotta [33] showed that an isothermal surface strip (width $2a$ and length L) on top of a substrate (width λ and length L) with semi-infinite thickness and insulated sides imposes a strip spreading resistance (R_{c-s}) equal to:

$$R_{c-s} = \frac{1}{\pi kL}\frac{1}{sin\left(\frac{\pi}{2}\sqrt{\frac{A_r}{A_a}}\right)} = \frac{1}{\pi kL}\frac{1}{sin\left(\frac{\pi}{2}\sqrt{\frac{2a}{\lambda}}\right)} \approx \frac{2}{\pi^2 kL}\sqrt{\frac{\lambda}{2a}} \quad (9)$$

Where the simplification on the right-hand side of Equation 9 is valid for $\lambda \gg 2a$. Since Equation 9 represents a geometry that is thermally insulated on the sides, it also represents a single unit cell of periodically arranged parallel strips. Thus, the total contact resistance presented by n_s such strip heat sources that conduct heat in parallel scales with R_{c-s}/n_s. Substituting Equations 7, 8, and 9

as well as multiplying by the apparent area yields the expected functional form of the contact resistance between a finger and a flatter, harder object for a unit area of the interface ($R_{c-s1}^{"}$ in units of m^2KW^{-1}):

$$R_{c-s1}^{"} \sim \frac{2A_a}{\pi^2 kLn_s\sqrt{\frac{2a}{\lambda}}} \sim \frac{2A_a}{\pi^2 kLn_s\sqrt{\frac{2a}{\lambda}}} \sim \frac{1.4}{k}\frac{\Delta}{m}\left(\frac{\Delta}{\lambda}\right)^{\frac{1}{4}}\left(\frac{E^*}{\bar{p}}\right)^{\frac{1}{4}} \tag{10}$$

Where $m \approx 4\Delta/\lambda$ is an approximate slope of a single ridge on the wavy surface. Recognizing that $\Delta \approx \sigma$, $\bar{p} \sim P$, $E^* = 2G/(1-\nu) \approx 4G$ (for an ideal incompressible material), there are two of these resistances in series (i.e. $1/k \to 2/k_s$), and that fourth root of the ridge aspect ratio (based on values from the finger surface scan $(\Delta/\lambda)^{1/4} \approx (10\ \mu m/500\ \mu m)^{1/4} \approx 1/3$) is nearly a constant yields the expanded functional form of PM's correlation:

$$R_{c-s}^{"} \sim R_{c-PM}^{"} \sim \frac{1}{k_s}\frac{\sigma}{m}\left(\frac{G}{P}\right)^{\frac{1}{4}} \tag{11}$$

Where this expanded version explicitly includes k_s and m as in the CMY model, on which PM based their correlation. Naturally, a real finger surface can depart from the parallel ridge idealization. Nerveless, scale analysis also reveals that for a smooth solid in contact with an elastic two-dimensional wavy surface (i.e. periodic sinusoidal bumps) functional form of Equation 11 also applies, albeit with minor alteration of exponential coefficient from 1/4 to 1/3 (see derivation in Supplemental Material). Consequently, despite its empirical roots, the PM correlation can be referred to as a model for finger-object contact resistance, since its form can be derived from first principles. Next, this notion is further supported by comparing the PM model against experimental measurements.

Comprehensive experimental measurements of finger contact resistance as a function of applied pressure, where all relevant parameters (σ, m, k, etc.) are reported, are not readily available in literature. Consequently, it is difficult to directly test applicability of the PM model. Instead, its

applicability is first evaluated here by modelling and reanalyzing the work of Ho and Jones [27]. Along with all relevant parameters, these authors measured the temporal evolution of a finger temperature during a 10 s contact with a cool and smooth barium fluoride crystal under a contact force, F, ranging from 0.1 to 2 N. Through direct measurements, the authors correlated F (in N) to apparent area (A_a in mm^2) as $A_a = 15.062\ln(F) + 170.31 \pm 20$. Given that $P = F/A_a$, the authors measured contact resistance from 0.7 to 11 kPa of contact pressure. Because of the short duration of the contact (thermal penetration for skin during a 10 s contact is $\sqrt{\alpha_{skin}t} \approx 1$ mm, where α_{skin} is the thermal diffusivity of skin), skin can be modelled as an isotropic semi-infinite body. Consequently, the temperature on the surface of the skin during this short contact (T_{skin}) can be predicted using a simple closed-form formula [27]:

$$T_{skin}(t) = \frac{A}{B}\left\{1 - e^{\alpha_{skin}B^2 t} erfc\left[B\sqrt{\alpha_{skin}t}\right]\right\} + T_{skin}(0) \quad (12)$$

Where $A = (T_{obj}(0) - T_{skin}(0))/R_c k_{skin}$ and $B = (1 + (k\rho c_p)_{skin}^{0.5}/(k\rho c_p)_{obj}^{0.5})/R_c k_{skin}$ while ρ and c_p stand for density and specific heat of the materials. To compare the experimental and theoretical finger temperatures, contact resistances must be calculated using CMY and PM models with material parameters (see Table 1) as well as $T_{obj}(0)$=299 K and $T_{skin}(0)$=306.3 K specified by Ho and Jones [27]. Figure 2a compares contact resistances calculated using the reported value range as a function of applied pressure. Both R''_{c-CMY} and R''_{c-PM} are within the expected range of 0.001 to 0.01 m^{2}KW^{-1} and follow comparable decreasing trend [7,9,27,12–19]. However, since $G_{skin} \approx 0.41$ kPa [31] and PM model has an 1/4 exponent, R''_{c-PM} decreases faster and nearly saturates around 0.002 m^{2}KW^{-1} past a contact pressure of 5 kPa. In contrast, the skin microhardness ($H_{skin} = 122.5$ kPa [34]) is much higher and CMY model has an exponent of 0.95, consequently R''_{c-CMY} decays slower and does not saturate until pressure reaches about 30 kPa. It is also worthwhile noting that due to the lower exponent, the large variation of measured

G_{skin} ($\pm$25 %) results in only about $\pm$6% variation in the value of R''_{c-PM}. At $P < 2.5$ kPa, R''_{c-CMY} is equal to or significantly larger than R''_{c-PM}. Above this pressure, R''_{c-CMY} continues to decrease far below R''_{c-PM} to 0.00175 m^2KW^{-1}, 0.001 m^2KW^{-1}, and 0.0005 m^2KW^{-1} at P of 5 kPa, 10 kPa, and 20 kPa, respectively. This trend in contact resistance is reflected in Figure 2b where, exactly replicating Ho and Jones simulations [27], using the CMY model with Equation 12 results in 1 to 2 K under prediction of skin temperature decrease at the end of contact when P is below 2.5 kPa, and about 1 K over prediction above this pressure. In contrast, the plot in Figure 2b shows that results of using the PM model with Equation 12 agree well with experimental data over the entire pressure range.

Table 1. Thermal properties of skin and BaF_2 [27,31] as well as aluminum, marble, and wood [20,35] (in the case of the latter upper value of thermal conductivity was from [35] was used). Since values in italic were not reported, the typical range reported in literature was used instead [36–39]. The reported uncertainty range corresponds to 68% confidence interval.

Material	Skin	BaF_2	Aluminum	Marble	Wood
Thermal Conductivity, k, $Wm^{-1}K^{-1}$	0.37	11.7	238	2.9	0.23 to 0.4
Density, ρ, kgm^{-3}	1000	4890	2700	2700	675
Specific Heat, c_p, $Jkg^{-1}K^{-1}$,	3770	410	917	881	3156
Thermal Diffusivity, α, $10^6 m^2s^{-1}$	0.098	5.9	0.96	1.2	0.1
RMS roughness, σ, µm	21.7±2	0.008	*1 to 6*	*5 to 30*	*5 to 30*
Microhardness, H, kPa	122.5±5.8	-	-	-	-
Effective Shear Modulus, G, kPa	0.41±0.1	-	-	-	-
Surface Asperity Slope, Δa, rad	0.3±0.03	0.009	*0.01 to 0.3*	*0.01 to 0.3*	*0.01 to 0.3*

The significant improvement in prediction of the finger contact resistance using the PM model is further highlighted by assessing skin surface temperature throughout the entire contact period. For simplification, here only the average values of skin properties reported in Table 1 are used in calculations. Figure 2c shows that using PM model (solid lines) rather than CMY model (dashed

lines) along with Equation 12 predicts a significantly smaller dependence of the skin temperature range on applied pressure. For example, when increasing pressure from 0.73 to 10.9 kPa, use of CMY model with Equation 12 predicts a skin temperature decrease of 4 to 5 K. In contrast, use of PM model with Equation 12 predicts a temperature decrease of only about 1 K, which closely agrees with the experimentally observed 0.5 to 1 K range shown in Figure 2d (which includes about 0.2 K uncertainty from the sensor). However, in both theoretical cases the initial rate of decrease of the temperature upon contact with the colder object is under predicted as compared to the measured values. This temporal feature could be partially explained by the set of thermal properties of skin utilized by Ho and Jones [27]. In particular, the authors used skin thermal diffusivity of $\alpha_{skin} = 9.8\times10^{-8}$ m^2s^{-1} in their calculations, while values up to $\alpha_{skin} = 1.2\times10^{-7}$ m^2s^{-1} can be found in other references [40].

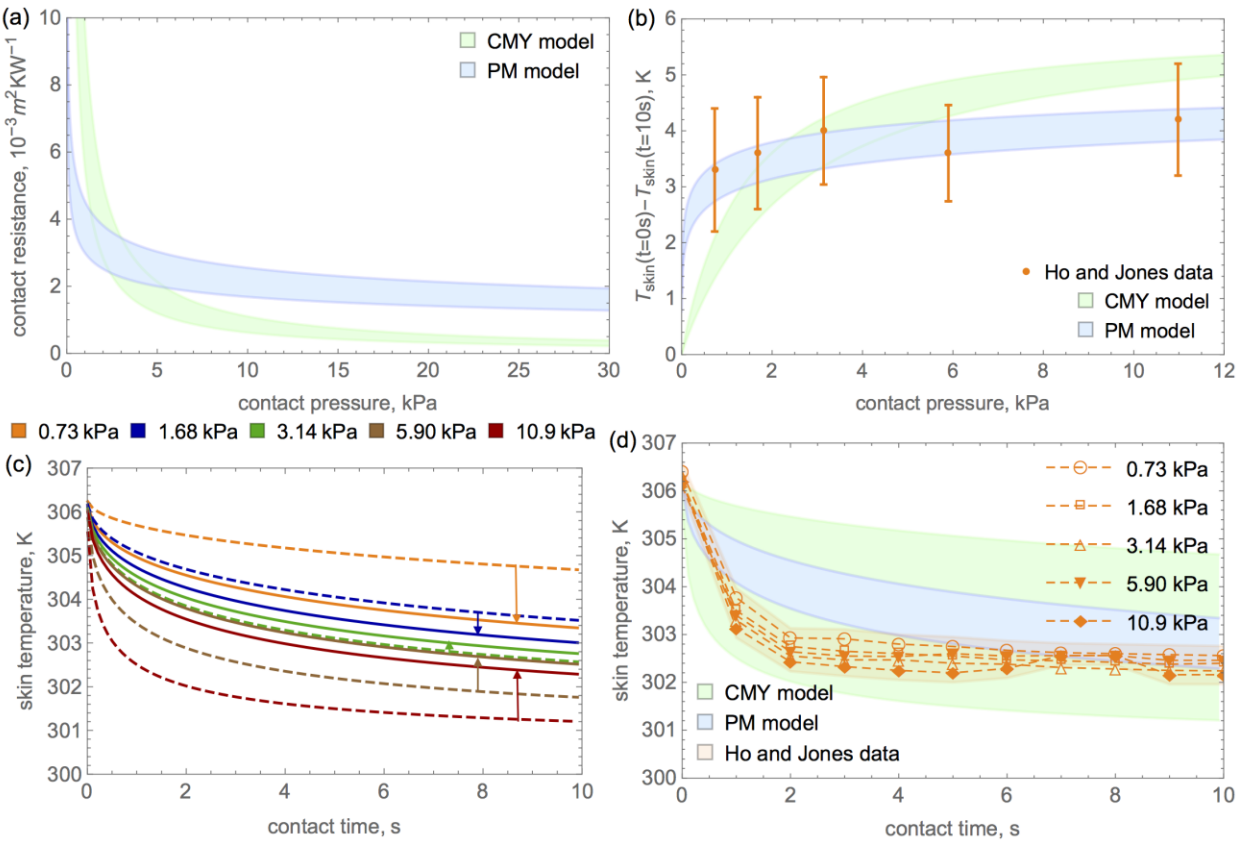

Figure 2. (a) Comparison between thermal contact resistance of finger and barium fluoride crystal interface calculated using CMY model (Equation 5) and PM model (Equation 6) and (b) comparison between experimentally measured (adapted from Ho and Jones [32]) and analytically predicted difference between finger temperature at the beginning and end of the 10 s contact period for contact pressure in the range of 0.78 to 11 kPa, (c) temporal evolution of the finger temperature during the contact calculated using average properties in reported in Table 1 and closed-form expression in Equation 12 and CMY model (dashed lines) or PM model (solid lines) contact resistance models (arrows are used as visual guides to highlight the difference between the two), and (d) lower and upper limits of the values in (c) along with Ho and Jones experimental data [32].

To further test the applicability of the PM model, the theoretical predictions of finger contact resistance are compared with another experimental data set reported by Maamir *et al.* [20] for fingers in contact with aluminum, marble, and wood surfaces. Unfortunately, these authors did not report apparent contact areas and surface roughness of skin or samples (or any details on sample preparation), therefore several assumptions must be made to calculate the contact resistance. To start with, Ho and Jones' [27] correlation for A_a as a function of F is adopted to determine that the 0.25 to 10 N force range tested by Maamir *et al.* [20] corresponds to about 1 to 50 kPa pressure range. While this range is much broader than the first test case of 0.7 to 11 kPa discussed above, this pressure range is comparable to one reported by Galie *et al.* (up to 35 kPa) [41]. Since most metal production methods (e.g. milling, grinding, polishing, lapping, extruding, cold rolling, etc.) produce a surface roughness below 6 μm [36], the surface roughness of aluminum plate is assumed to be significantly smaller than that of skin and the effective surface roughness is dominated by the latter value, i.e. $\sigma \approx \sigma_{skin}$. With this assumption and substitution of the range of skin properties indicated in Table 1 into Equations 5 and 6, Figure 3a shows that PM model predictions are in remarkably good agreement with data for finger contact with an aluminum plate from Maamir *et al.* [20]. This agreement is not surprising since Equation 6 was obtained by fitting data on comparably soft materials and metal surface interfaces where $k_2 \gg k_1$.This notion, however, starts to be questionable for marble ($k_{marble} = 2.9$ $Wm^{-1}K^{-1}$) and is not valid for wood ($k_{wood} = 0.23$ to 0.4 $Wm^{-1}K^{-1}$ [35] that is comparable to $k_{skin} = 0.37$ $Wm^{-1}K^{-1}$). To account for this discrepancy, k_s, as suggested by scale analysis, is utilized instead of k_1 in Equation 6. Furthermore, according to literature typical marble and wood surface finishing methods can produce surface roughness of up to 30 μm (if one takes into account about 50% potential increase due to aging for marble) [37–39,42]. When this possible variation is taken into account, the plot in Figure 3b shows that almost

all data points for finger-marble interface fall within the contact resistance value range predicted by PM model, but are mostly outside of the range predicted by CMY model. In case of the finger-wood contact, however, the plot in Figure 3c shows that experimental points are within and close to the lower bound of the range of PM model and, for low pressures, are also within the range of CMY model. The most troubling aspect revealed by plot in Figure 3c is the large spread of calculated contact resistance. The sensitivity analysis presented in Supplemental Material reveals that this large spread predominantly results from sensitivity of the PM and CMY models to the substrate's thermal conductivity, if it is below 1 $Wm^{-1}K^{-1}$. Specifically, above this value of the substrate's thermal conductivity, k_s is equal to twice the thermal conductivity of skin (see Figure S1a in Supplemental Material). Consequently, the applicability of PM model appears to be limited to modeling of finger contact with substrates with thermal conductivity above 1 $Wm^{-1}K^{-1}$ and excludes substrates such as wood or plastics. The sensitivity analysis also shows that substrate surface roughness values below about 8 μm have no impact on R''_{c-PM}, consequently can be considered smooth (i.e. Equation 6 with roughness of skin can be utilized). However, if the substrate surface is rougher, the assumptions behind the scale analysis and PM's measurements break down, therefore further theoretical and experimental work is necessary to establish model for contact resistance in such cases.

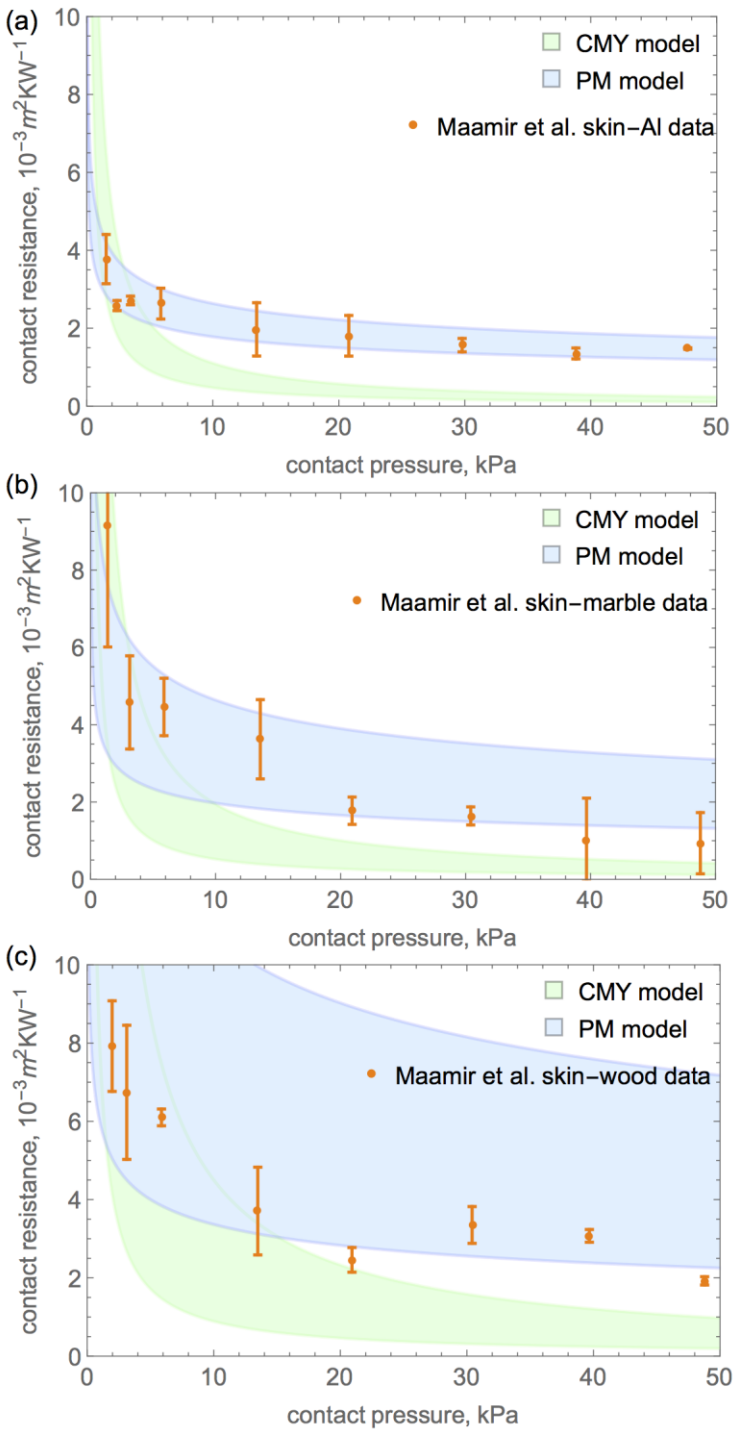

Figure 3. Comparison between theoretical predictions of thermal contact resistance by CMY and PM models including experimental data on finger contact with (a) aluminum, (b) marble, and (c) wood surfaces from Maamir *et al.* [16]. The shaded areas correspond to possible range of properties indicated in Table 1 and specified in text.

In summary, scale analysis as well as comparison between experimental data from literature with CMY and PM models shows that the latter model should be utilized to calculate the thermal contact resistance at the finger-object interface. Scale analysis revealed that the main difference between the functional forms of CMY and PM models (i.e. exponent decrease from about 1 to 1/4) is rooted in the switch of the assumed contact deformation mode from plastic to elastic. In the former case, the number of contact points increases with pressure, while their mean size remains roughly unchanged leading to $R''_{c-CMY} \sim 1/P$. In the latter case, the number of contact points is constant, while their area increases with applied pressure leading to $R''_{c-PM} \sim (1/P)^{\frac{1}{4}}$ and $R''_{c-PM} \sim (1/P)^{\frac{1}{3}}$ for periodic wavy ridge and periodic wavy bump surfaces, respectively. Current results also denote that the PM model is applicable for finger contact with stiff substrates with roughness below about 8 μm that have thermal conductivity above 1 $Wm^{-1}K^{-1}$ (e.g. aluminum, BaF_2, and marble), but only provides an order of magnitude estimate for materials with lower conductivity (e.g. wood and plastics). However, due to rarity of published comprehensive data on finger-object contact resistance, further experimental work is necessary to provide definite evidence on the general applicability of PM model for interfaces between skin and hard objects with moderate thermal conductivity and surface roughness.

There are two key implications the results discussed above highlight. First, owing to the low modulus value of skin and the one fourth power exponent in PM model, the value of the contact resistance decreases quickly with increasing pressure and nearly saturates at relatively mild pressures. For example, for finger contact with a highly conductive material, contact resistance decreases to 0.003 m^2KW^{-1} at 2.5 kPa and settles around 0.002 m^2KW^{-1} if more than 5 kPa is applied. It is worthwhile mentioning that this saturation prediction not only matches well with Maamir *et al.* [20] data, but also with the value that Alkhwaji *et al.* [43] recently inferred from

simulations and experimental data. Thus, if just a mild pressure of a few kilopascals is applied, the contact resistance can be assumed to be nearly pressure independent and equal to 0.002 to 0.003 m^2KW^{-1}. For rougher or less thermally conductive objects contact resistance saturation with pressure is also likely to occur, albeit with different threshold pressure and saturation values (see Figure 3b and 3c). Naturally, if an interfacial grease or liquid (e.g. sweat) is present, then contact resistance will be different from these saturation values. Second, current results imply that the low frequency shear modulus, rather than the microhardness, should be used as the characteristic mechanical property of skin for contact resistance calculations. This implication is beneficial since shear modulus values are readily available in literature or can be objectively measured for any material ranging from gels to diamond. In contrast, the relevant microhardness guideline CMY use (i.e., the pressure obtained from indentation tests using an indenter on the size of the microcontacts) leaves a lot of room for subjective interpretation and simply cannot be obtained for soft materials [29]. Also, knowing that $G_{skin} \approx 410$ Pa [31] (although this value could be affected by individual subject characteristics and location on the body), one can safely assume that in most cases finger is the softer of the two materials, thus its mechanical properties should be used to calculate the contact resistance. It is important to note, however, that it is not clear when this assumption breaks down and how to calculate contact resistance between skin and a comparably soft material. This is an interesting area for future research and will increasingly become important in thermal design of mobile, epidermal, and wearable electronics that often interface with the user through a soft exterior [1–5,44]. Lastly, current results support the recent idea of Sripada et al.[4], that a silicone gel finger can reasonably well mimic the thermal response of its human counterpart to short contact (a few seconds) with colder or hotter hard objects. To provide the closest match to finger, the shear modulus of the used silicone gel and surface roughness should also be close to that of the skin.

Acknowledgements

This work was in part supported by the National Science Foundation through award number CBET #1724452. The author would like to thank Mr. Akshay Phadnis, Mr. Praveen Kotagama, Mr. Kenneth C. Manning, and Prof. Robert Wang from ASU for commenting on the manuscript. Lastly, the author would like to remind Ms. Agata Renata Rykaczewski that, well, I told you not to touch it, it was hot!

Disclosure of potential conflicts of interest

No potential conflicts of interest were disclosed.

Supplemental Material includes full nomenclature, scale analysis of the two-dimensional wavy surface contact, parameter sensitivity analysis of the PM and CMY models, and optical profilometry procedure.

References

[1] H.-N. Ho, *Material recognition based on thermal cues: Mechanisms and applications*, Temperature 5 (2018), pp. 36–55.

[2] H. Zhang and A. Hedge, *Overview of Human Thermal Responses to Warm Surfaces of Electronic Devices*, J. Electron. Packag. 139 (2017), pp. 30802.

[3] S.K. Roy, An equation for estimating the maximum allowable surface temperatures of electronic equipment, in Semiconductor Thermal Measurement and Management Symposium (SEMI-THERM), 2011 27th Annual IEEE, 2011, pp. 54–62.

[4] A. Sripada, M. Rohlfing, R. Vijaendreh, B. Spetzler, R. Abdulhamid, A. Porras et al., *Use of a Gel Finger to Feel the Skin Temperatures of a Smartphone*, J. Electron. Packag. 138 (2016), pp. 31001.

[5] Y. Yin, Y. Cui, Y. Li, Y. Xing and M. Li, *Thermal management of flexible wearable electronic devices integrated with human skin considering clothing effect*, Appl. Therm. Eng. (2018), .

[6] Y. Li, Y. Gao and J. Song, *Recent advances on thermal analysis of stretchable electronics*, Theor. Appl. Mech. Lett. 6 (2016), pp. 32–37.

[7] L.A. Jones and H.-N. Ho, *Warm or cool, large or small? The challenge of thermal displays*, IEEE Trans. Haptics 1 (2008), pp. 53–70.

[8] J.-J. Cabibihan, D. Joshi, Y.M. Srinivasa, M.A. Chan and A. Muruganantham, *Illusory sense of human touch from a warm and soft artificial hand*, IEEE Trans. Neural Syst. Rehabil. Eng. 23 (2015), pp. 517–527.

[9] H.-N. Ho and L.A. Jones, Thermal model for hand-object interactions, in Haptic Interfaces for Virtual Environment and Teleoperator Systems, 2006 14th Symposium on, 2006, pp. 461–467.

[10] F. Suarez, D.P. Parekh, C. Ladd, D. Vashaee, M.D. Dickey and M.C. Öztürk, *Flexible thermoelectric generator using bulk legs and liquid metal interconnects for wearable electronics*, Appl. Energy 202 (2017), pp. 736–745.

[11] F. Suarez, A. Nozariasbmarz, D. Vashaee and M.C. Öztürk, *Designing thermoelectric generators for self-powered wearable electronics*, Energy Environ. Sci. 9 (2016), pp. 2099–2113.

[12] A.Z. Şahin, *an Experimental Study on the Initiation and Growth of Frost Formation on a*

Horizontal Plate, Exp. Heat Transf. 7 (1994), pp. 101–119.

[13] B. Saggin, M. Tarabini and G. Lanfranchi, *A device for the skin–contact thermal resistance measurement*, IEEE Trans. Instrum. Meas. 61 (2012), pp. 489–495.

[14] W.M.B. Tiest, An experimentally verified model of the perceived'coldness' of objects, in EuroHaptics Conference, 2007 and Symposium on Haptic Interfaces for Virtual Environment and Teleoperator Systems. World Haptics 2007. Second Joint, 2007, pp. 61–65.

[15] W.M.B. Tiest and A.M.L. Kappers, *Thermosensory reversal effect quantified*, Acta Psychol. (Amst). 127 (2008), pp. 46–50.

[16] W.M.B. Tiest and A.M.L. Kappers, *Tactile perception of thermal diffusivity*, Attention, perception, Psychophys. 71 (2009), pp. 481–489.

[17] W.M.B. Tiest, *Tactual perception of material properties*, Vision Res. 50 (2010), pp. 2775–2782.

[18] M. Gabardi, D. Chiaradia, D. Leonardis, M. Solazzi and A. Frisoli, A High Performance Thermal Control for Simulation of Different Materials in a Fingertip Haptic Device, in International Conference on Human Haptic Sensing and Touch Enabled Computer Applications, 2018, pp. 313–325.

[19] Y. Osawa and S. Katsura, Thermal impedance control for thermal rendering technique, in Industrial Electronics Society, IECON 2015-41st Annual Conference of the IEEE, 2015, pp. 4015–4020.

[20] F. Maamir, M. Guiatni, Y. Morsly and A. Kheddar, Pso algorithm based thermal contact resistance estimation for variable force hand/object interaction, in Control and Automation (MED), 2014 22nd Mediterranean Conference of, 2014, pp. 499–504.

[21] M.G. Cooper, B.B. Mikic and M.M. Yovanovich, *Thermal contact conductance*, Int. J. Heat Mass Transf. 12 (1969), pp. 279–300.

[22] M.M. Yovanovich, *Thermal contact correlations*, AIAA Pap. 81 (1982), pp. 83–95.

[23] A. Bejan and A.D. Kraus, *Heat Transfer Handbook*, Vol. 1, John Wiley & Sons, 2003.

[24] M. Bahrami, J.R. Culham and M.M. Yovanovich, *Modeling thermal contact resistance: a scale analysis approach*, J. Heat Transfer 126 (2004), pp. 896–905.

[25] R. Holm, *Electrical contacts handbook*, Splinger 15 (1958), pp. 1023–1029.

[26] M.M. Yovanovich, *Four decades of research on thermal contact, gap, and joint resistance in microelectronics*, IEEE Trans. components Packag. Technol. 28 (2005), pp. 182–206.

[27] H.-N. Ho and L.A. Jones, *Modeling the thermal responses of the skin surface during hand-object interactions*, J. Biomech. Eng. 130 (2008), pp. 21005.

[28] S.K. Parihar and N.T. Wright, *Thermal contact resistance at elastomer to metal interfaces*, Int. Commun. heat mass Transf. 24 (1997), pp. 1083–1092.

[29] R.S. Prasher and J.C. Matayabas, *Thermal contact resistance of cured gel polymeric thermal interface material*, IEEE Trans. Components Packag. Technol. 27 (2004), pp. 702–709.

[30] R.S. Prasher and C.-P. Chiu, *Thermal Interface Materials*, in *Materials for Advanced Packaging*, Springer, 2017, pp. 511–535.

[31] B. Holt, A. Tripathi and J. Morgan, *Viscoelastic response of human skin to low magnitude physiologically relevant shear*, J. Biomech. 41 (2008), pp. 2689–2695.

[32] K.L. Johnson, *Contact Mechanics*, Cambridge university press, 1987.

[33] M.M. Yovanovich and E.E. Marotta, *Thermal spreading and contact resistances*, Heat Transf. Handb. 1 (2003), pp. 261–394.

[34] E.S. Dellon, K. Keller, V. Moratz and A.L. Dellon, *The relationships between skin*

hardness, pressure perception and two-point discrimination in the fingertip, J. Hand Surg. Am. 20 (1995), pp. 44–48.

[35] H. Thunman and B. Leckner, *Thermal conductivity of wood—models for different stages of combustion*, Biomass and Bioenergy 23 (2002), pp. 47–54.

[36] E. Oberg, F. D. Jones, H. L. Horton and H. H. Ryffel, *Machinery ' s Handbook*, 2000.

[37] N.P. Avdelidis, E.T. Delegou, D.P. Almond and A. Moropoulou, *Surface roughness evaluation of marble by 3D laser profilometry and pulsed thermography*, NDT E Int. 37 (2004), pp. 571–575.

[38] P. López-Arce, M.J. Varas-Muriel, B. Fernández-Revuelta, M.Á. de Buergo, R. Fort and C. Pérez-Soba, *Artificial weathering of Spanish granites subjected to salt crystallization tests: Surface roughness quantification*, Catena 83 (2010), pp. 170–185.

[39] E.A. Papp and C. Csiha, *Contact angle as function of surface roughness of different wood species*, Surfaces and Interfaces 8 (2017), pp. 54–59.

[40] R.C. Eberhart and A. Shitzer, *Heat Transfer in Medicine and Biology: Analysis and Applications*, Vol. 2, Springer Science & Business Media, 2012.

[41] J. Galie, H.-N. Ho and L.A. Jones, Influence of contact conditions on thermal responses of the hand, in EuroHaptics conference, 2009 and Symposium on Haptic Interfaces for Virtual Environment and Teleoperator Systems. World Haptics 2009. Third Joint, 2009, pp. 587–592.

[42] P. Vazquez and J.F. Alonso, *Colour and roughness measurement as NDT to evaluate ornamental granite decay*, Procedia Earth Planet. Sci. 15 (2015), pp. 213–218.

[43] A. Alkhwaji, B. Vick and T. Diller, *New mathematical model to estimate tissue blood perfusion, thermal contact resistance and core temperature*, J. Biomech. Eng. 134 (2012),

pp. 81004.

[44] M.D. Bartlett, N. Kazem, M.J. Powell-Palm, X. Huang, W. Sun, J.A. Malen et al., *High thermal conductivity in soft elastomers with elongated liquid metal inclusions*, Proc. Natl. Acad. Sci. 114 (2017), pp. 2143–2148.